Available online at www.eccomasproceedia.org
Eccomas Proceedia COMPDYN (2023) 3647-3659

ECCOMAS
Proceedia

COMPDYN 2023
9th ECCOMAS Thematic Conference on
Computational Methods in Structural Dynamics and Earthquake Engineering
M. Papadrakakis, M. Fragiadakis (eds.)
Athens, Greece, 12-14 June 2023

FEASIBILITY STUDY OF MICROTREMOR SIGNALS FOR STRUCTURAL HEALTH MONITORING ON REAL STEEL BUILDING STRUCTURES

Chih-chun Ou[1], and Jun Iyama[2]

[1] Graduate Student Researcher, Graduate School of Engineering, The University of Tokyo
7 Chome-3-1 Hongo, Bunkyo City, Tokyo, Japan 113-8654
moods0707@g.ecc.u-tokyo.ac.jp

[2] Associate Professor, Graduate School of Engineering, The University of Tokyo
7 Chome-3-1 Hongo, Bunkyo City, Tokyo, Japan 113-8654
iyama@arch1.t.u-tokyo.ac.jp

Abstract

Square hollow section (SHS) columns are widely used in many Asian countries such as Japan and China for the construction of low- and middle-rise steel buildings. Post-earthquake damage surveys and structural condition assessments of this common type of structure have attracted increasing attention in order to ensure business continuity. Many measuring instruments for structural health monitoring (SHM) of buildings such as accelerometers have been commercially available; however, measuring acceleration response alone does not allow for direct estimation of damage to individual structural members. Another potential structural health monitoring instrument is the strain gauge; however, it has very limited application in structures. This research aims to establish a method to evaluate the severity of structural damage by strain measurement under microtremor and ambient vibration. A 1-story steel frame was designed to examine the applicability of this method in real buildings. Steel base plates for columns are fixed to the concrete foundations by anchor bolts, whose loosening will be used to simulate different levels of structural damage. The strains measured directly from the anchor bolts showed to be very sensitive to the loosening of the bolts. In addition, the local stiffness observed from the lower part of the column, which has a smaller cross-sectional area, tends to be more significant compared to that measured from the upper part. The reduction of stiffness at the column base can be observed from the bending moment distribution under microtremor. In this research, the classification models were trained with different machine learning tools for structural damage assessment. In general, trained models can successfully classify the different damage states and the severity of the damage.

Keywords: Structural health monitoring, Damage detection, Steel frame structure, Strain measurement, Microtremor, Machine learning.

ISSN:2623-3347
Peer-review under responsibility of the organizing committee of COMPDYN 2023.
doi: 10.7712/120123.10668.20317

1 INTRODUCTION

Steel frames have been used all over the world due to the relatively well ductility compared to the concrete structures. However, during the 1995 Hyogo-ken Nambu earthquake in Japan, substantial damages were still observed [1][2]. Meanwhile, enterprises and factories suffered damage to their buildings and equipment, disrupting the supply chain and hitting the local economies of steel, automobiles, liquor brewing, and the chemical and footwear industries [3]. In the 1999 Chi-Chi earthquake in Taiwan, damage to the electronic component industry even temporarily caused a global crisis in computer production [4].

To ensure the business continuity and safety, structure health monitoring (SHM) has acquired increasing attentions and many measuring instruments have become commercially available. For example, many attempts have been made to apply accelerometers for SHM and the overall behavior of the structure can be monitored [5][6]. However, because changes in structural response behavior due to structural damage are usually very minor, measuring the acceleration solely tends to be difficult for evaluating the damage state of individual structural members [7][8]. Instead of evaluating the damage condition only by accelerometer, some studies have focused on the strain response under small vibration. Iyama et al. proposed a method using an index "local stiffness" including the strain response measured by the strain gauges attached to the beam flanges and the displacement measured by the displacement transducer; the results confirmed that this method is effective for fracture localization especially for buckling damage [9][10].

Steel column base plays an important role in transmitting the earthquake load from concrete base to the superstructure in the steel frame system. Therefore, the connection mechanism between the concrete part and the steel member has gained a lot of interest. Some studies have been made to clarify the mechanism of this connection [11]. Square hollow section (SHS) columns are widely used in many Asian countries such as Japan and China for the construction of low- and middle-rise steel buildings. In this research, a 1-story steel frame with SHS columns was designed to examine the applicability of this method in real buildings. Steel column base is fixed to the concrete foundations by anchor bolts, whose loosening will be used to simulate different levels of structural damage. Whenever a bolt is loosened, the test structure is manually shaken to apply small vibrations.

The strains measured directly from the anchor bolts are shown in this study. Comparisons were made between the local axial stiffness and local bending stiffness as measured from the upper and lower column sections. It is addressed how the distribution of bending moments changes as a result of the loosening of anchor bolts. These results suggest the possibility of a quantitative assessment of damage by strain measurements.

In recent years, machine learning has been applied to many areas of research, such as biotechnology and medical science, and many believe it has great potential for the SHM method [12]. In this research, the strain data measured under microtremor and small vibration was used as the training materials to build a model for damage condition classification of steel frame structures. For creating the training data set, the short-time Fourier transform can be used to convert the measured vibration data into a spectrogram. In addition to exploring the potential for structural damage assessment, the classification models were trained utilizing a variety of tools to make it simpler for more people to use and promote this approach.

2 EXPERIMENT OVERVIEW

2.1 Test setup

A 1-story steel frame was designed to examine the applicability of the proposed SHM method in real buildings. Figure 1 and 2 show the photograph and schematic, respectively, of the test structure. Each column can be separated into two parts: the 1500 mm lower part (□-150x150x12; b/t = 12.5) and the 2600 mm upper part (□-200x200x9; b/t = 22.2). Both two parts were manufactured using the material STKR400, which has the Young's modulus = 205000 N/mm^2; yielding strength = 245 N/mm^2; maximum strength = 400 N/mm^2. Each column was held in place by four anchor bolts illustrated in Figure 3. The loosening of these bolts is used to simulate the damage of column base.

Figure 1: Photograph of the test structure.

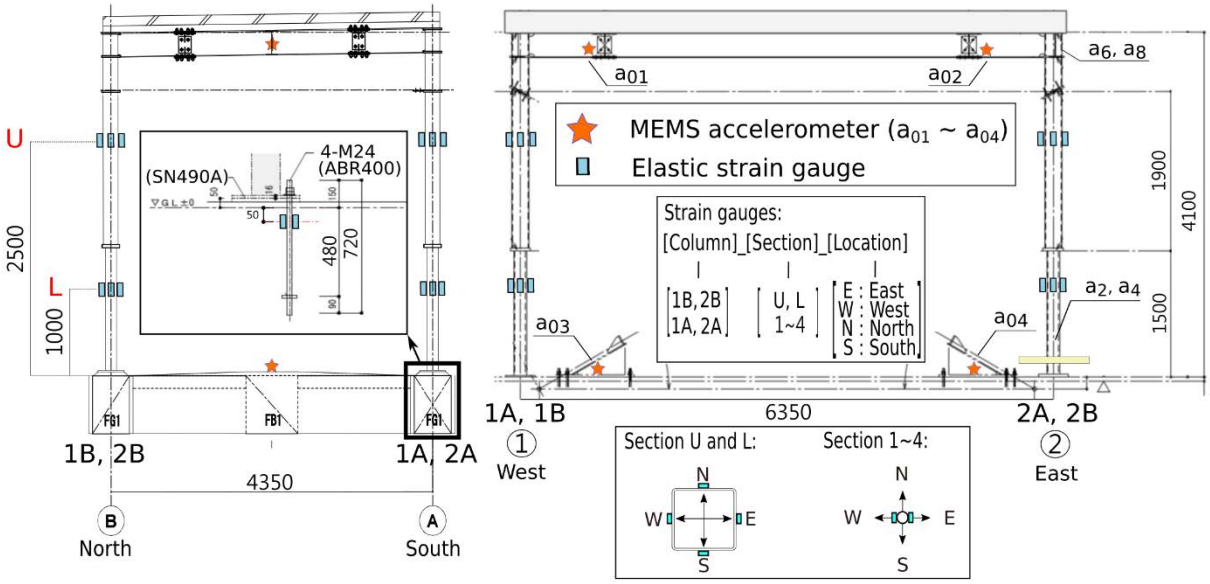

Figure 2: Test setup and measurement.

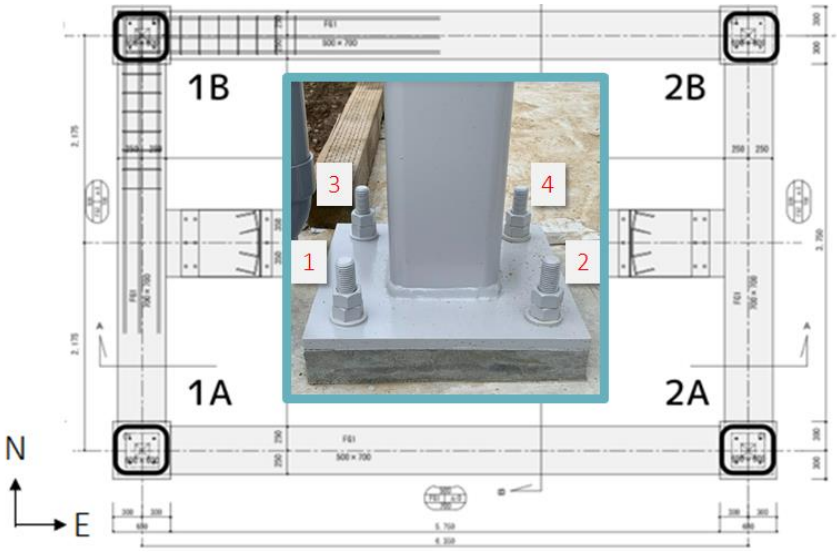

Figure 3: Structure plan view and the name of anchor bolts.

2.2 Data acquisition devices

The data acquisition was implemented using Raspberry Pi units as shown in Figure 4, which was used to collect the acceleration data and strain data during small vibration with a sampling rate up to 86 Hz for strain and 125 Hz for acceleration, respectively.

(a) Strain gauge units (b) Accelerometer unit

Figure 4: Raspberry Pi units.

3 DAMAGE DETECTION METHOD

3.1 Detection principle

In this paper, we aim to capture small response under microtremor before and after the damage occurred to capture changes in vibration characteristics.

Suppose a column suffers the horizontal displacement, d, at the top and accordingly the strain, ε_W and ε_E are occurred at the east and west sides of a certain section as shown in Figure 2. If the column is in an elastic state, d and ε are proportional. The ratio, $\frac{\varepsilon}{d}$, is hereinafter referred to as "local stiffness" and denoted by K_ε. This includes the "local axial stiffness", $K_{\varepsilon,a}$, and the "local bending stiffness", $K_{\varepsilon,b}$, that are illustrated in the equations bellow:

$$K_{\varepsilon,a} = \frac{\hat{\varepsilon}_{i,W} + \hat{\varepsilon}_{i,E}}{2\hat{d}} \quad ; \quad K_{\varepsilon,b} = \frac{\hat{\varepsilon}_{i,W} - \hat{\varepsilon}_{i,E}}{2\hat{d}} \tag{1}$$

Here, ^ represents the Fourier transform to a certain parameter. For the location of the displacement measurement, it is desirable to select a location the displacement at which is considered strongly correlated to the measured strain. Therefore, the displacement, d, was measured using the accelerometers placed at the top (a_{01}, a_{02}) and bottom (a_{03}, a_{04}) of the test specimen, as shown in Figure 2. Because $K_{\varepsilon,a}$ and $K_{\varepsilon,b}$ have similar physical meaning with axial force and bending moment, respectively, when the distribution of bending moment changed due to the damage of column base, it is expected that similar change can be captured by strain measurement even under microtremor as shown in Figure 5.

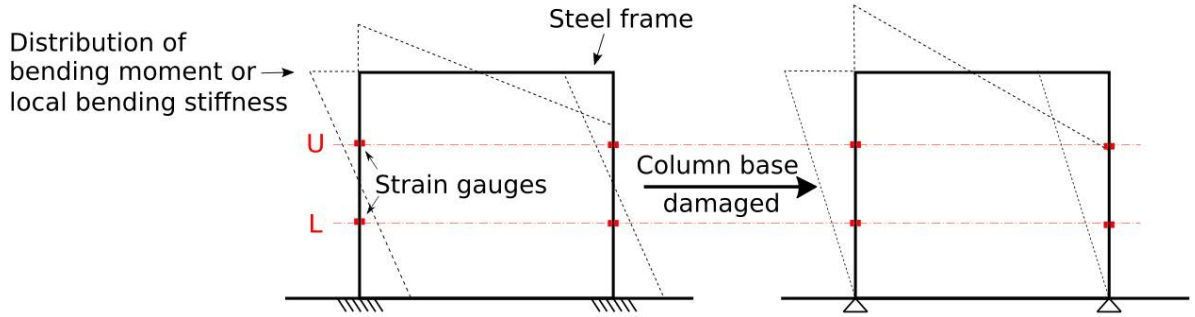

Figure 5: Concept of the damage detection method based on strain measurement.

3.2 Test procedure

Table 1 shows the test procedure. The capital, M, represent microtremor which is applied manually by man power before and after each step. The name of the steps is written as the column name followed by the bolt number and the process. For example, 1A -1 loosened means the bolt number 1 of column 1A was loosened. After the M16 step, all bolts in four column bases were loosened. From the M17 step, the bolts started to be fastened one by one until the final step.

Step.	Status	Step.	Status	Step.	Status
M00	Intact	M12	1B -3 loosened	M24	2A -3 fastened
M01	1A -1 loosened	M13	2B -1 loosened	M25	1B -1 fastened
M02	1A -4 loosened	M14	2B -4 loosened	M26	1B -4 fastened
M03	1A -2 loosened	M15	2B -2 loosened	M27	1B -2 fastened
M04	1A -3 loosened	M16	2B -3 loosened	M28	1B -3 fastened
M05	2A -1 loosened	M17	1A -1 fastened	M29	2B -1 fastened
M06	2A -4 loosened	M18	1A -4 fastened	M30	2B -4 fastened
M07	2A -2 loosened	M19	1A -2 fastened	M31	2B -2 fastened
M08	2A -3 loosened	M20	1A -3 fastened	M32	2B -3 fastened (Intact)
M09	1B -1 loosened	M21	2A -1 fastened		
M10	1B -4 loosened	M22	2A -4 fastened		
M11	1B -2 loosened	M23	2A -2 fastened		

Table 1: Test procedure.

3.3 Measurement

Figure 6 shows an example of the time history of acceleration and strain measured by the instrument that the attachment position is shown in Figure 2 while the lower graphs show an enlarged view of the upper graphs. The measured time history and spectrum of the MEMS accelerometers and strain gauges show almost identical shapes, indicating successful measurement.

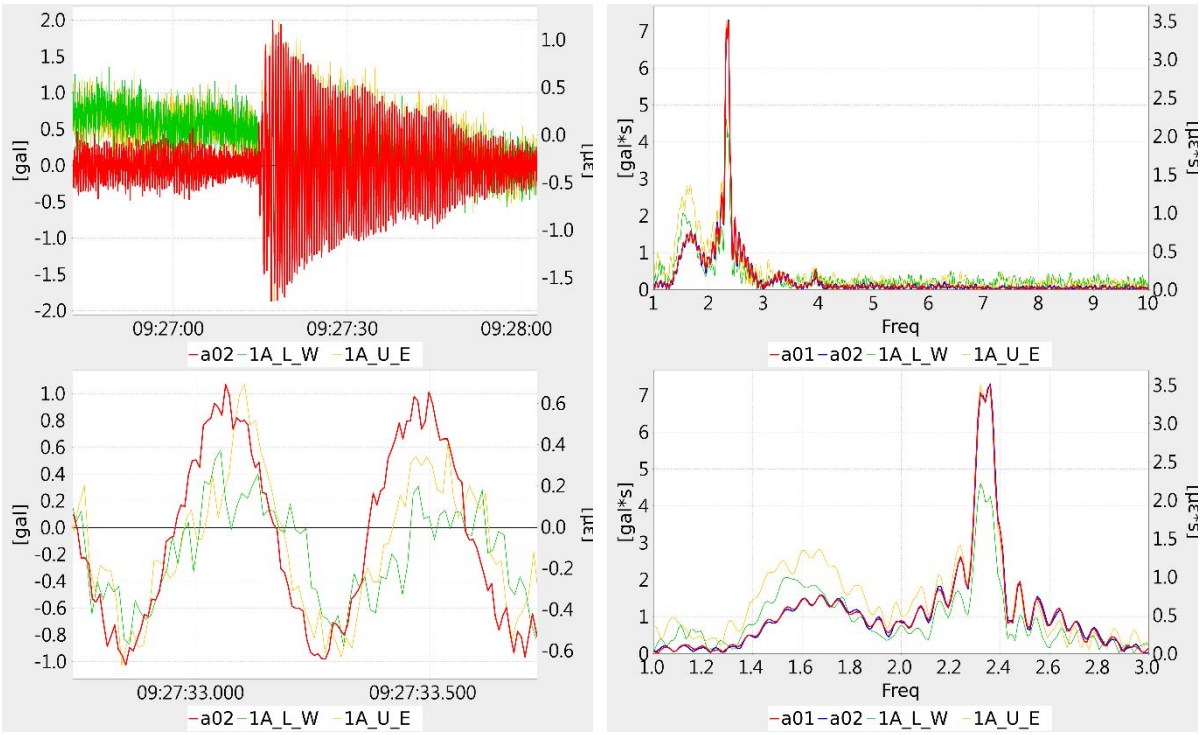

Figure 6: Recorded time history and spectrum

3.4 Training materials for machine learning

The strain data measured from all 64 strain gauges are used to create the training dataset for machine learning. Figure 7 shows an example of generating the training data of the column 1A.

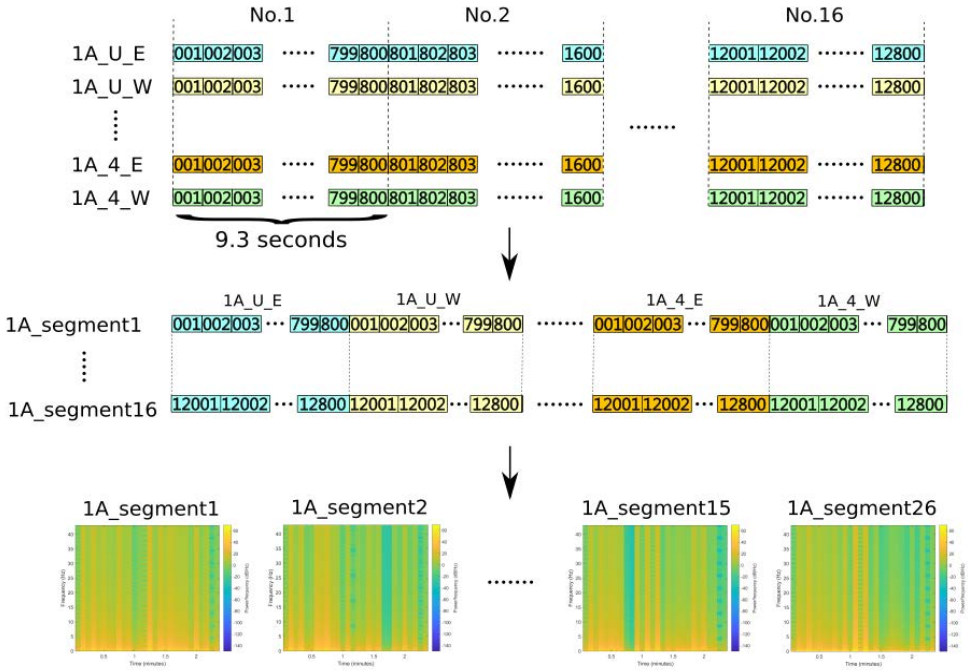

Figure 7: Concept of generating training dataset

As shown in Figure 7. The strain was measured starting from the time when the vibration was applied and last for a duration of 150 seconds. Each data set is composed of strain data

measured from 16 strain gauges on 1 column. The strain data measured in 150 seconds is split into 16 segments and numbered. All segments with the same number will then be connected to form a training data. Finally, the training data will be converted into spectrograms by means of a short-time Fourier transform form to train the model.

4 TEST RESULT

4.1 Strain measurement on anchor bolts

Figure 8 shows an example of the time history of the axial strain on the anchor bolts. The horizontal axis shows the time, while the vertical axis shows the average of strain measured on the two sides of the anchor bolt, respectively.

According to Figure 8(a) and (b), the strain gauges attached to the anchor bolts are sensitive to changes in the loosening and fastening of the bolts. Due to systematic errors, the strain data needs to be zeroed manually. In this diagram, the strain measured right before the tightening of the nut is set to zero. Therefore, in order to monitor damage to anchor bolts through strain time histories, continuous measurements are necessary to capture the changes.

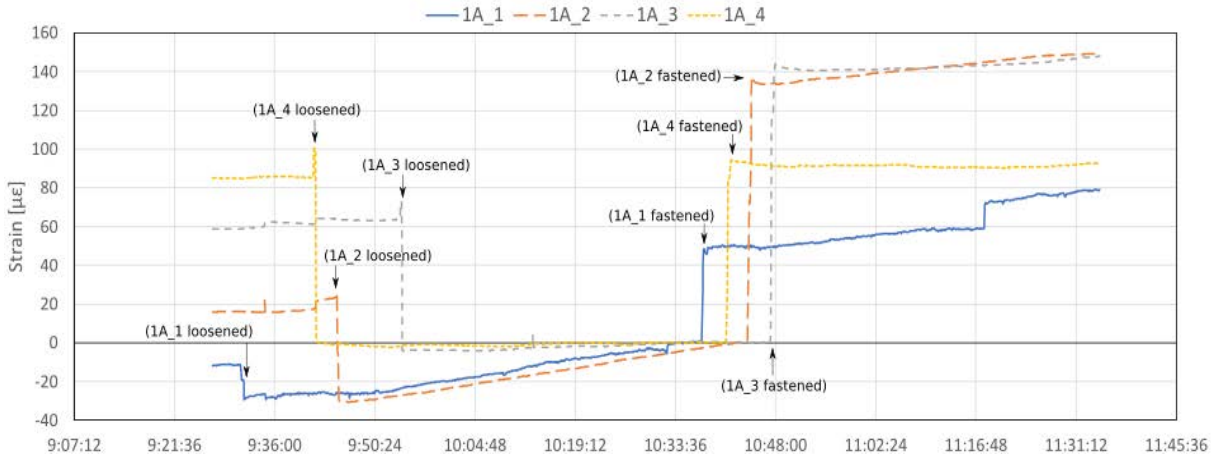

(a) Column 1A

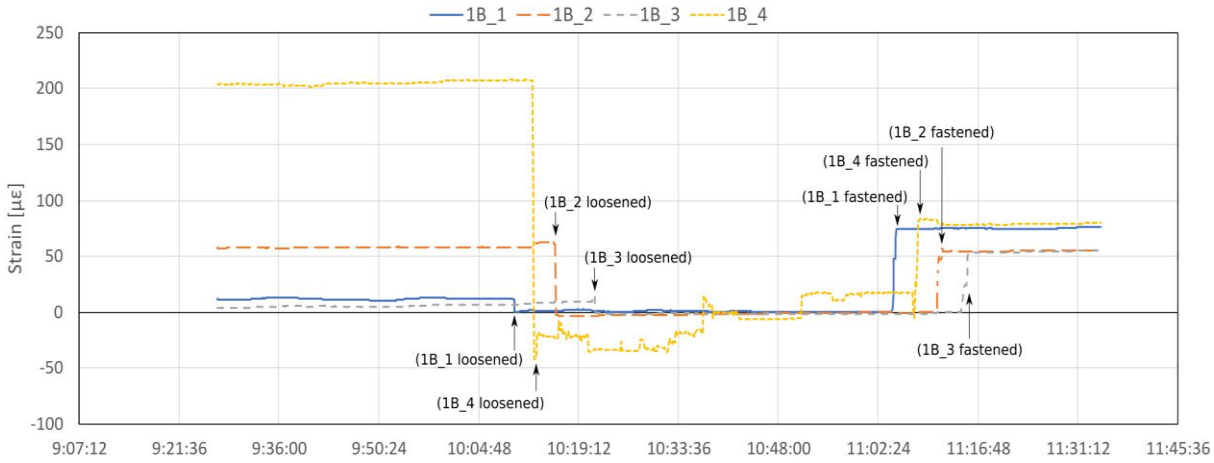

(b) Column 1B

Figure 8: Change in strain measured from individual anchor bolt

4.2 Local stiffness of column sections

Local stiffness of the upper and lower section of the column 1A calculated using Eq. (1) are illustrated in Figure 9. Unlike the time history of the axial strain on the anchor bolt, the local axial stiffness ($K_{\varepsilon,a}$) remains almost constant. On the other hand, the local bending stiffness ($K_{\varepsilon,b}$) is relatively sensitive to changes in the loosening and tightening of the bolt especially in the lower section, which can be used as a potential indicator for damage detection.

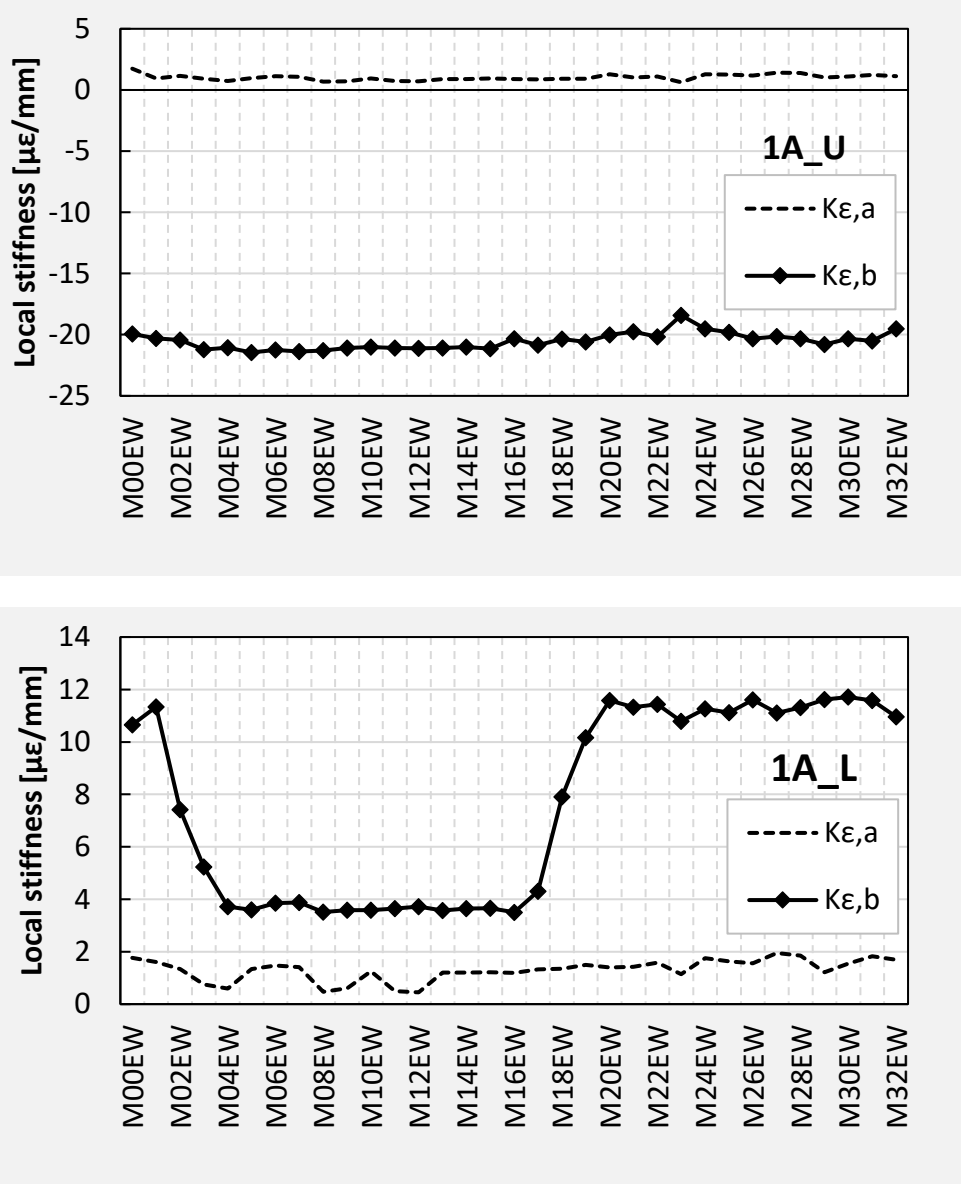

Figure 9: Local stiffness measured on sections 1A_U and 1A_L

4.3 Bending moment distribution

Because the local stiffness does not consider the different sectional properties between the upper part and lower part of the column, it may also be preferable to use the bending moment distribution. In general, the bending moment can be written as Eq. (2):

$$M = EI\varphi = EI \times \frac{\varepsilon_{i,W} - \varepsilon_{i,E}}{H} = \frac{EI}{H}\left(\varepsilon_{i,W} - \varepsilon_{i,E}\right) \tag{2}$$

Using the concept of local stiffness, the bending moment normalized by displacement can be calculated as Eq. (3):

$$\widehat{M} = \frac{EI}{H} \times \frac{\hat{\varepsilon}_{i,W} - \hat{\varepsilon}_{i,E}}{2\hat{d}} = \frac{EI}{H} \times K_{\varepsilon,b} \tag{3}$$

Figure 10 shows the bending moment distribution of the column 1A calculated using Eq. (3). The values at the top and bottom sections are calculated by extrapolation. A reduction in the bending moment at the bottom of the column can be observed, indicating a reduction in the stiffness at the column base.

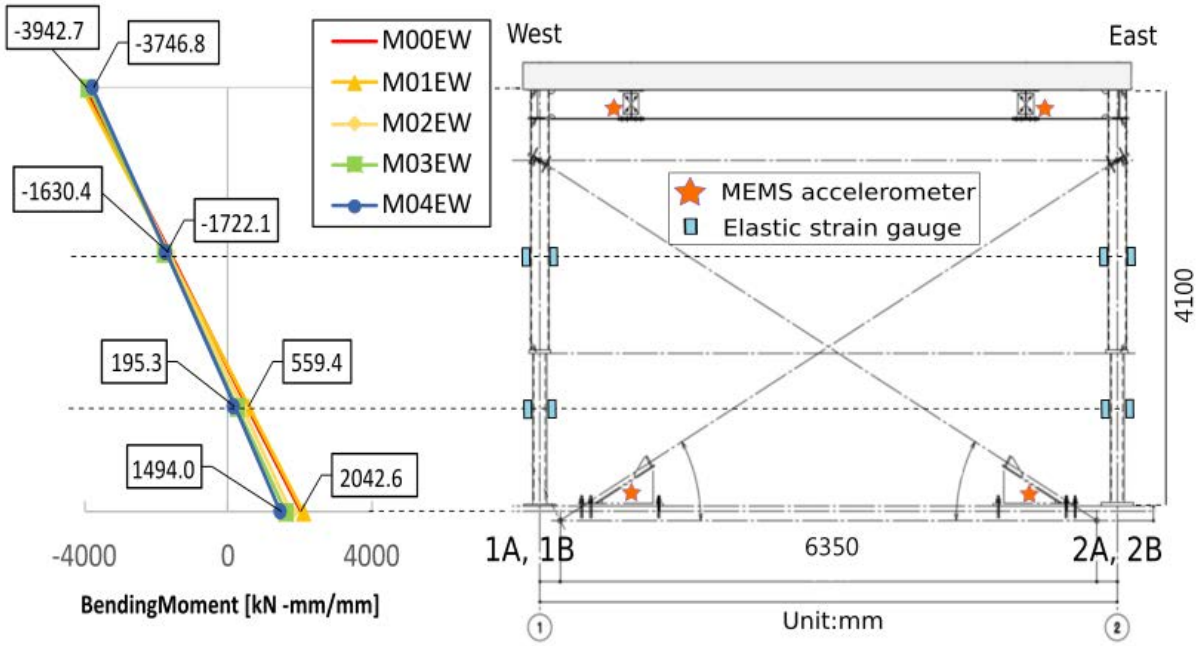

Figure 10: Bending moment distribution of the column 1A

4.4 Damage classification using machine learning

In this research, the amount of total data sets is relatively small. Therefore, spectrograms created from all four columns are combined and classified into five damage classes: 1. No bolts have been loosened; 2. One bolt has been loosened; 3. Two bolts have been loosened; 4. Three bolts have been loosened; and 5. All bolts have been loosened. For each damage class, 128 spectrograms were used as the image samples and the batch size was set as 16.

Figure 11 and Figure 12 illustrate the training result using Teachable Machine where the learning rate was set as 0.0005. The default validation rate is 0.15, which cannot be changed. The trained model performed well, and the training time was less than 30 seconds. The training values are close to the test values, meaning that there is less overfitting. Furthermore, the model can successfully identify extreme situations (Class 1 and Class 5), but it performs poorly when classifying images from Class 3. In conclusion, thanks to the powerful cloud server, the teachable machine can easily classify different damage cases with minimal training time.

Figure 11: Accuracy and loss per epoch trained by Teachable Machine

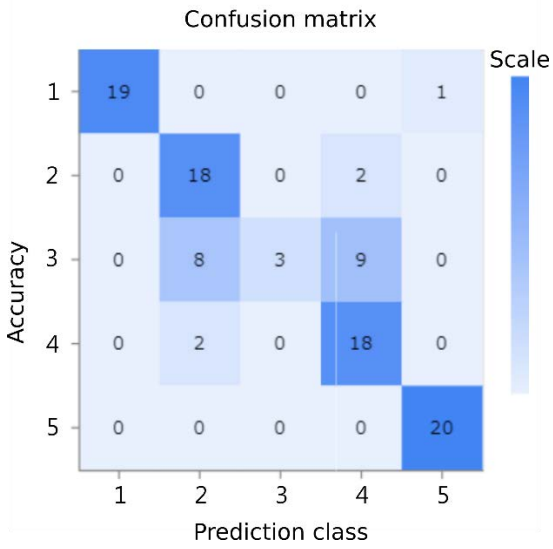

Figure 12: Confusion matrix created by Teachable Machine

Figure 13 and Figure 14 illustrate the training result using the Deep Network Designer in MATLAB. While the Teachable Machine is based on MobileNet, a pretrained image recognition network, in this research, we also use a pretrained image network called NasNet-Mobile which has 913 layers and 1071 connections. Due to the small amount of data, the validation frequency was set to 5 iterations. The initial learning rate was set as 0.01 while the drop ratio was set as 0.1.

According to the result, the trained model performed well; however, it takes about 3 hours to train using the 11th Generation Intel Core i7. Because the training values are close to the test values, there is less overfitting. In addition, similar to the result made by Teachable Machine, while the model is capable of identifying extreme situations (Class 1 and Class 5), it performs relatively poorly when classifying images from Class 2 to Class 3. However, compared to Teachable Machine, because the network created in MATLAB can be manually tuned, it has the potential to train a better model if the parameters are properly adjusted.

In conclusion, it has been demonstrated that training damage classification models using raw strain data is efficient and only requires a limited amount of data processing. Once the

technology matures, the level of technological expertise required for structural health monitoring will significantly decrease.

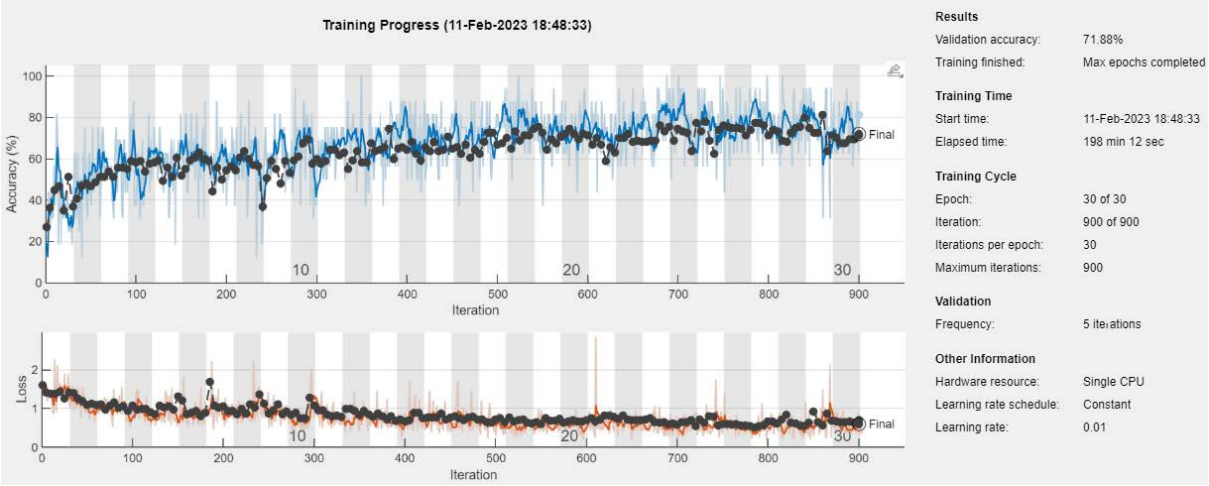

Figure 13: Accuracy and loss per epoch trained by NasNet-Mobile

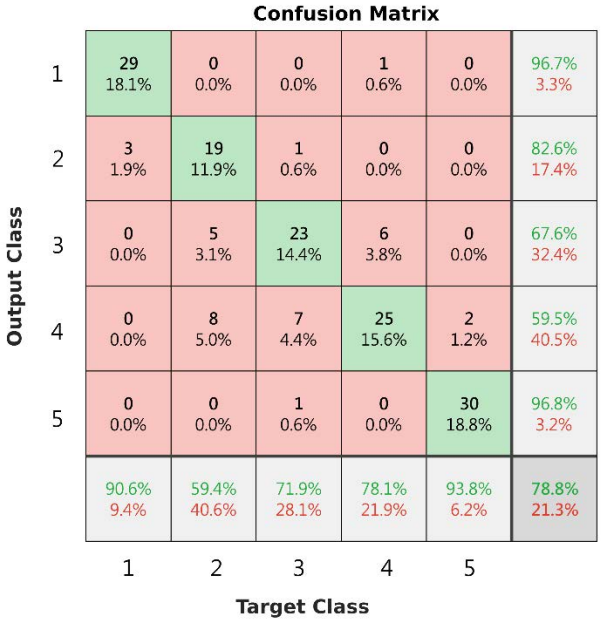

Figure 14: Confusion matrix created by the model trained by NasNet-Mobile

5 CONCLUSIONS

- The strain gauges attached to the anchor bolts are sensitive to changes in the loosening and fastening of the bolts.
- In order to monitor damage to anchor bolts through strain time histories, continuous measurements are necessary to capture the changes.
- Compared to the local axial stiffness ($K_{\varepsilon,a}$), the local bending stiffness ($K_{\varepsilon,b}$) measured on the column surface is relatively sensitive to changes in the loosening and tightening of the bolt especially in the lower section

- Using the concept of local stiffness, the bending moment distribution normalized by displacement shows a trend of reduction at the bottom of the column, indicating a reduction in the stiffness at the column base.
- For both Teachable Machine and NasNet-Mobile, the trained model performed well with an accuracy of 70-80%; However, the Teachable Machine is more time saving while NasNet-Mobile implemented using MATLAB is more customizable.
- Once the proposed methods mature, the level of technological expertise required for structural health monitoring will significantly decrease.

REFERENCES

[1] Scawthorn, C., & Yanev, P. I. (1995). 17 January 1995, Hyogo-ken Nambu, Japanese earthquake. Engineering Structures, 17(3), 146-157.

[2] Watanabe, E., Sugiura, K., Nagata, K., & Kitane, Y. (1998). Performances and damages to steel structures during the 1995 Hyogoken-Nanbu earthquake. Engineering Structures, 20(4-6), 282-290.

[3] Maruya H (2008) Significance and Economic Effect of Business Continuity Plan, Gyosei Co., p.2, (in Japanese).

[4] Lee Y, Watanabe K, Li WS (2019) Enhancing Regional Disaster Resilient Trade and Investment – Business Continuity Management. In: Murayama Y, Velev D, Zlateva P. (eds) Information Technology in Disaster Risk Reduction. ITDRR 2017. IFIP Advances in Information and Communication Technology, vol. 516. Springer, Cham. https://doi.org/10.1007/978-3-030-18293-9_10

[5] Brownjohn JMW (2003) Ambient vibration studies for system identification of tall buildings. Earthquake Eng Struct Dyn 32(1): 71–95.

[6] Yousefianmoghadam S, Behmanesh I, Stavridis A, Moaveni B, Nozari A, Sacco A (2018) System identification and modeling of a dynamically tested and gradually damaged 10‐story reinforced concrete building. Earthq Eng Struct Dyn 47: 25‐47.

[7] Kubota J, Suzuki Y, Suita K Sawamoto Y, Kiyokawa T, Koshika N, Takahashi M (2017) Experimental study on the collapse process of an 18-story high-rise steel building based on the large-scale shaking table test. In: 16th World Conference on Earthquake Engineering, Santiago, Chile, 9–13 January 2017.

[8] Kubota J, Takahashi M, Sawamoto Y, Suzuki Y, Koetaka Y, Iyama J, Nagae T (2018) Collapse behavior of 18-story steel moment frame on shaking table test. J. Struct. Constr. Eng. AIJ 83(746): 625–635 (in Japanese).

[9] Iyama J (2017) Detection of damage and fracture of steel members based on micro strain measurement. In: 9th International Symposium on Steel Structures, Jeju, Korea, 1–4 November 2017.

[10] Iyama J, Hasegawa T, Nakagawa H, Kaneshiro Y (2019) Beam end fracture detection of two-story steel frame based on micro strain measurement under microtremor. In: 12th Pacific Structural Steel Conference, Tokyo, Japan, 15–17 December 2019.

[11] Sato, K., & Ikarashi, K.: Local buckling behavior and evaluation method for structural performance of square hollow section members under bending shear force. Journal of Structural and Construction Engineering 82(731), 123-133 (2017) (in Japanese)

[12] Wang, S., Shi, J., Ye, Z., Dong, D., Yu, D., Zhou, M., ... & Tian, J. (2019). Predicting EGFR mutation status in lung adenocarcinoma on computed tomography image using deep learning. European Respiratory Journal, 53(3).